Ligament-bone interaction in a three-dimensional model of the knee

Ligament-Bone Interaction in a Three-Dimensional Model of the Knee

L. Blankevoort

R. Huiskes

Biomechanics Section, Institute of Orthopaedics, University of Nijmegen, Nijmegen, The Netherlands

In mathematical knee-joint models, the ligaments are usually represented by straight-line elements, connecting the insertions of the femur and tibia. Such a model may not be valid if a ligament is bent in its course over bony surfaces, particularly not if the resulting redirection of the ligament force has a considerable effect on the laxity or motion characteristics of the knee-joint model. In the present study, a model for wrapping of a ligament around bone was incorporated in a three-dimensional mathematical model of the human knee. The bony edge was described by a curved line on which the contact point of the line element representing a ligament bundle was located. Frictionless contact between the ligament bundle and the bone was assumed. This model was applied to the medial collateral ligament (MCL) interacting with the bony edge of the tibia. It was found that, in comparison with the original model without bony interactions, the bony edge redirected the ligament force of the MCL in such a way that it counterbalanced valgus moments on the tibia more effectively. The effect of the bony interaction with the MCL on the internal-external rotation laxity, however, was negligible.

Introduction

In previous knee-joint models, ligaments have been represented by nonlinear elastic line elements which directly connect the insertions by straight lines (Crowninshield et al., 1976; Wismans et al., 1980; Wismans, 1980; Andriacchi et al., 1983; Essinger et al., 1989). A ligament may, however, wrap around a bone. For instance, a direct straight-line connection between the tibial and femoral insertions of the medial collateral ligament (MCL) runs through the articular surfaces of the tibia and the femur. If the MCL is represented by straight line elements, the ligament-bone interaction by the wrapping of a ligament around a bony surface, causing a realignment of the ligament force, is neglected. The question then is whether the redirection of a ligament force affects the laxity or motion characteristics of the knee-joint model. Hefzy and Grood (1983) proposed a model for the wrapping of ligaments around bones. Results with respect to its effect on the behavior of a knee-joint model have not been reported.

In the present study, a model for ligament-bone interaction was incorporated into a three-dimensional mathematical model of the human knee joint. The model of the wrapping of the MCL around the bony edge of the tibia was based on the assumptions and simplifications proposed by Hefzy and Grood (1983). The effect of this ligament-bone interaction on the restraining function of the MCL for axial and valgus rotations was evaluated.

Contributed by the Bioengineering Division for publication in the JOURNAL OF BIOMECHANICAL ENGINEERING. Manuscript received by the Bioengineering Division August 10, 1990; revised manuscript received March 30, 1991.

Methods

General Description of the Knee Model. The same basic assumptions and simplifications as reported by Wismans et al. (1980) were used in developing the present knee model. The knee model describes the quasistatic behavior of the tibiofemoral joint for moderate loading conditions, whereby the femur is considered to move relative to the tibia. The geometry of the tibial and femoral articular surfaces, and the insertion locations of the ligaments were based on geometry measurements (Huiskes et al., 1985; Meijer et al., 1988; Blankevoort et al., 1991a) on a knee specimen for which a set of experimental kinematic data was available (Blankevoort et al., 1988). Although the menisci do have a certain role in determining the laxity characteristics of the knee (Bargar et al., 1980; Markolf et al., 1981; Blankevoort et al., 1984), the menisci are not included because of the complexity of incorporating them in the present mathematical formulation of the knee model. This model also accounts for deformable articular contact, whereby friction is assumed to be negligible (Blankevoort et al., 1991b). The model describes the position of the femur relative to the tibia for a given configuration of external loads and kinematic constraints. A subsequent series of joint positions simulates knee motion.

The position of the femur relative to the tibia is found by solving the equilibrium equations for forces and moments acting on the femur

$$\mathbf{f}_e + \mathbf{f}_r + \mathbf{f}_l + \mathbf{f}_c = 0, \tag{1a}$$

$$\mathbf{m}_e + \mathbf{m}_r + \mathbf{m}_l + \mathbf{m}_c = 0, \tag{1b}$$

in which $\mathbf{f}_e$ and $\mathbf{m}_e$ are the externally applied forces and mo-

ments, $\mathbf{f}_r$ and $\mathbf{m}_r$ are the forces and moments required to maintain the applied kinematic restraints, $\mathbf{f}_l$ and $\mathbf{m}_l$ are the forces and moments caused by ligament tensions, and $\mathbf{f}_c$ and $\mathbf{m}_c$ are the forces and moments generated by articular contact. The equilibrium equations are expressed relative to the tibial coordinate system. The externally applied forces and moments are assumed to be constant relative to the tibial coordinate system, whereas the other forces and moments are functions of the translations and rotations of the femur relative to the tibia. The equilibrium equations are solved through a Newton-Raphson procedure, in which analytical partial derivatives of the equations with respect to the motion parameters are used.

Relative Joint Position and Kinematic Constraints. Two Cartesian coordinate systems are introduced for motion description, a space-fixed system of the tibia and a body-fixed system of the femur. The x_1-axis points anteriorly, the x_2-axis points medially and the x_3-axis points proximally. Each position of the femur is then characterized by a translation of the origin and three rotations about the axes of either the body-fixed coordinate system or the space-fixed coordinate system. Introducing the translation vector $\mathbf{a}$ from O (the origin of the tibial coordinate system) to $\hat{O}$ (the origin of the femoral coordinate system) and the rotation matrix $\mathbf{R}$, the position of a material point $\hat{P}$ on the femur can be described by the vector $\mathbf{p}$ from O to $\hat{P}$ and the vector $\mathbf{R}\cdot\hat{\mathbf{p}}$ from $\hat{O}$ to $\hat{P}$. They are related by

$$\mathbf{p}=\mathbf{a}+\mathbf{R}\cdot\hat{\mathbf{p}}. \tag{2}$$

At the reference position where the coordinate systems coincide, $\hat{\mathbf{p}}$ is the position vector of the material point, $\mathbf{a}$ is a zero vector and $\mathbf{R}$ is the identity matrix. The reference position is defined for the knee joint in extension. In this reference position, the origins of the tibial and the femoral coordinate systems are located 15 mm proximal relative to the insertion of the posterior bundle of the anterior cruciate ligament (pAC) on the tibia, in the approximate region where the helical axes for flexion motions are located (Blankevoort et al., 1990).

For describing the rotations, the convention of the Joint Coordinate System as proposed by Grood and Suntay (1983) is used. This rotation convention defines the rotations about the bodyfixed axes of the moving tibia relative to the fixed femur in the sequence flexion, varus and internal rotation. Since the femur is moving relative to the tibia in the present model, a compatible rotation convention is then given by rotations about the body-fixed axes of the femur, provided that the rotations and the rotation sequence are reversed: external rotation (x_3-axis), valgus (x_1-axis) and extension (x_2-axis) (Woltring, 1990).

One or more of the translations or rotations may be prescribed and their values can be substituted in the force, moment and contact equations. In order to maintain applied kinematic constraints, constraint forces and moments have to be introduced

$$\mathbf{f}_r=\sum_1^m -\sigma_i\boldsymbol{\alpha}_i, \tag{3a}$$

$$\mathbf{m}_r=\sum_1^m -\sigma_i\boldsymbol{\beta}_i, \tag{3b}$$

in which $\mathbf{f}_r$ is the constraint force acting on the femur, $\mathbf{m}_r$ is the constraint moment about $\hat{O}$, σ_i denotes the magnitude of the constraint load, and m is the number of kinematic constraints. The vectors $\boldsymbol{\alpha}_i$ and $\boldsymbol{\beta}_i$ are determined by the derivatives of the translation vector and the rotation matrix with respect to the translation and the rotation components, respectively (Appendix). The values for σ_i follow from the solution of the system of equilibrium equations.

Ligaments. The ligaments are modelled by two or more line elements representing different fiber bundles in the ligament. The ligament bundles are assumed to be nonlinear elastic. This means that the tension in a ligament bundle is only a function of its length L or strain ϵ. Ligament strain is defined by

$$\epsilon=(L-L_0)/L_0, \tag{4}$$

in which L_0 is the zero-load length of a ligament.

Let $\mathbf{s}$ and $\mathbf{R}\cdot\hat{\mathbf{s}}$ denote the position vectors describing the insertions of a ligament bundle at tibia and femur, respectively (Fig. 1). Using Eq. (2), the unit vector pointing along the line of action of the ligament bundle as represented by a straight line, is given by

$$\mathbf{v}=(\mathbf{a}+\mathbf{R}\cdot\hat{\mathbf{s}}-\mathbf{s})/\|\mathbf{a}+\mathbf{R}\cdot\hat{\mathbf{s}}-\mathbf{s}\|, \tag{5}$$

in the case that a ligament is represented as a straight line not wrapping around a bone. The force $\mathbf{f}_j$ acting on the femur and the moment $\mathbf{m}_j$ about $\hat{\mathbf{O}}$, which are caused by the tensile force in ligament bundle j is then expressed by

$$\mathbf{f}_j=-f_j(\epsilon_j)\mathbf{v}_j, \tag{6a}$$

$$\mathbf{m}_j=(\mathbf{R}\cdot\hat{\mathbf{s}}_j)\times\mathbf{f}_j, \tag{6b}$$

in which $\mathbf{f}_j(\epsilon_j)$ is the tensile force in the ligament bundle. This force is either positive or zero. If ℓ is the number of ligament bundles modelled, the total force $\mathbf{f}_l$ acting on the femur and moment $\mathbf{m}_l$ about $\hat{\mathbf{O}}$ generated by the tensile forces in the ligament bundles are found by summation over all ligament bundles, yielding

$$\mathbf{f}_l=\sum_1^\ell -f_j(\epsilon_j)\mathbf{v}_j, \tag{7a}$$

$$\mathbf{m}_l=\sum_1^\ell (\mathbf{R}\cdot\hat{\mathbf{s}}_j)\times\mathbf{f}_j. \tag{7b}$$

For the interaction of a line element with a bony edge of the tibia, it is assumed that the ligament fiber bundle is bent at a point on a spatial curve fixed to the tibia (Fig. 1). The position vector of the contact point p on the curve is given by

$$\mathbf{p}=\mathbf{p}(\lambda)=[p_1(\lambda),\ p_2(\lambda),\ p_3(\lambda)]', \tag{8}$$

in which λ is the curve position parameter. The ligament length is the sum of two line segments, one running from the tibial insertion to point p on the edge, and the second from p to the

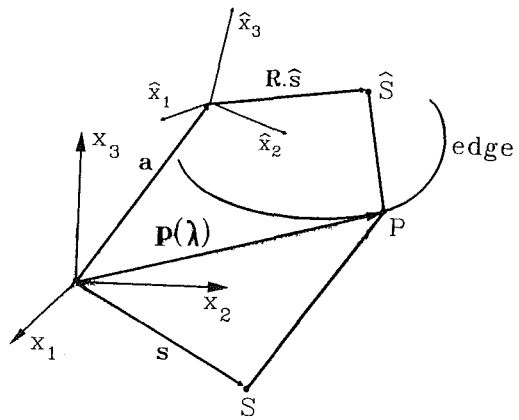

Fig. 1 Schematic representation of the coordinate systems and the model for ligament bone interaction. (x_1,x_2,x_3) is attached to the tibia and is assumed to be space-fixed. $(\hat{x}_1,\hat{x}_2,\hat{x}_3)$ is attached to the femur and is assumed to be body-fixed. The vector a describes the translation of the body-fixed origin relative to the space-fixed origin. The bony edge is modelled by a spatial circular curve. The ligament bundle is modelled by a line element which is divided into two segments, one from the tibial insertion S to the contact point P with the edge and the second from P to the femoral insertion $\hat{S}$, S is described by the vector s and $\hat{S}$ is described by $(a+R\cdot\hat{s})$. The contact point P on the edge is described by the vector p. p is a function of the position parameter λ.

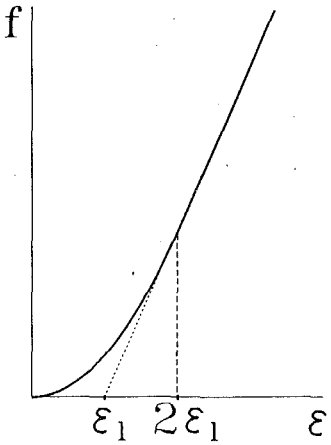

Fig. 2 The force-strain (f – ε) relationship for the elastic line elements modelling the ligament fiber bundles. A quadratic curve is assumed for strains below $2\epsilon_1$ and a linear relation is assumed for strains higher than $2\epsilon_1$.

femoral insertion. The ligament length is thus a function of the curve position parameter λ

$$L = L_1 + L_2, \tag{9a}$$

$$(L_1)^2 = (\mathbf{p}(\lambda) - \mathbf{s}) \cdot (\mathbf{p}(\lambda) - \mathbf{s}), \tag{9b}$$

$$(L_2)^2 = (\mathbf{a} + \mathbf{R} \cdot \hat{\mathbf{s}} - \mathbf{p}(\lambda)) \cdot (\mathbf{a} + \mathbf{R} \cdot \hat{\mathbf{s}} - \mathbf{p}(\lambda)), \tag{9c}$$

The unit vector along the line of action of the femoral force is denoted by

$$\mathbf{v} = (1/L_2)(\mathbf{a} + \mathbf{R} \cdot \hat{\mathbf{s}} - \mathbf{p}(\lambda)), \tag{10}$$

and the unit vector of the tibial force by

$$\mathbf{w} = (1/L_1)(\mathbf{p}(\lambda) - \mathbf{s}). \tag{11}$$

The position parameter λ is found by minimizing L, which is evaluated through

$$(\partial L_1/\partial\lambda) + (\partial L_2/\partial\lambda) = 0. \tag{12}$$

Substitution of the derivatives of L_1 (9*b*) and L_2 (9*c*) into λ, and using Eqs. (10) and (11), yields

$$(\mathbf{w} - \mathbf{v}) \cdot (\partial \mathbf{p}/\partial\lambda) = 0. \tag{13}$$

This equation is solved to find the position parameter λ for each iteration in the Newton-Raphson procedure. With the position parameter λ, the length and strain of a line element are obtained by using (9) and (4). The expressions for the force $\mathbf{f}_j$ and moment $\mathbf{m}_j$ are then the same as equations (6).

The function $f_j(\epsilon_j)$ is assumed to be nonlinear for low strains and linear for strains higher than a certain level (Fig. 2) (Wismans, 1980)

$$f = \tfrac{1}{4} k\epsilon^2/\epsilon_l \quad 0 \le \epsilon \le 2\epsilon_l, \tag{14a}$$

$$f = k(\epsilon - \epsilon_l) \quad \epsilon > 2\epsilon_l, \tag{14b}$$

$$f = 0 \quad \epsilon < 0, \tag{14c}$$

in which f is the tensile force in a line element, k is the ligament stiffness, and ϵ is the strain in the ligament calculated from its length L and the zero-load length L_0 (4). At the reference (extension) position of the joint, the initial strain in a ligament bundle is given by the parameter ϵ_r. This parameter determines the zero-load length of a ligament bundle if the reference length L_r of the bundle is known

$$L_0 = L_r/(\epsilon_r + 1). \tag{15}$$

The medial collateral ligament (MCL) was modelled to wrap around the medial bony edge of the tibia. This bony edge was approximated by a spatial circular curve which runs through three points located on the bone. It was assumed that the ligament-edge contact remained present throughout the model simulation and that no loosening occured. This can be checked through graphical inspection at the extremes of the simulated motions. The presence of the bony edge increased the reference length of the MCL slightly for the reference position of the joint in the kinematic experiment, where the joint was positioned in extension with no external loads. In the two models with and without the medial bony edge, the reference lengths of the MCL were thus slightly different, but the same ligament stiffnesses and reference strains were chosen (Table 1). The stiffness values of the ACL, PCL, and MCL were derived from the linear elastic modulus for the knee ligaments as reported by Butler et al. (1986), and the cross-sectional geometry from Danylchuk et al. (1975). The stiffness of the LCL was chosen from the model of Andriacchi et al. (1983), and that of the two bundles of the deep part of the MCL were estimated from Wismans (1980). The stiffness was equally divided over the different line elements of each ligament. The ligament reference strains in the model were estimated on the basis of a comparison of the internal and external rotation laxities between the model and the experimentally obtained values from the specimen of which the ligament insertion locations and the articular geometry were obtained (Blankevoort et al., 1991b). The linear strain limit ϵ_l was set at 0.03 (Butler et al., 1986).

Table 1 The parameters of the line elements modeling the ligaments. k is the linear stiffness and ϵ_r is the reference strain for the joint in extension

Ligament	Ligament bundle	k [N]	ϵ_r
anterior cruciate	aAc	5000	0.06
	pAC	5000	0.10
posterior cruciate	aPC	9000	−0.24
	pPC	9000	−0.03
lateral collateral	aLC	2000	−0.25
	sLC	2000	−0.05
	pLC	2000	0.08
medial collateral	aMC	2750	0.04
	iMC	2750	0.04
	pMC	2750	0.03
medial capsule	aCM	1000	−0.18
	pCM	1000	−0.04

Articular Contact. The model for deformable articular contact describes a thin linear elastic layer on a rigid foundation, as described by Blankevoort et al. (1991b). The contact model is a first-order approximation for the relation between normal surface stress σ_n and the normal surface displacement u_n

$$\sigma_n = S(u_n/b), \tag{16}$$

with

$$S = \frac{(1-\nu)E}{(1+\nu)(1-2\nu)}, \tag{17}$$

where b is the thickness of the cartilage layer, E is the elastic modulus, and ν is the Poisson's ratio. In the present model where two bodies are in contact, the material properties and the thickness of the cartilage of the tibia and the femur are assumed to be constant over the articular surface. The parameter b in equation (16) is then equal to the sum of the cartilage thicknesses of the opposing surfaces, and u is the sum of the tibial and femoral surface displacements.

The compressive contact force on the femur $\mathbf{f}_c$ and contact moment $\mathbf{m}_c$ about $\hat{\mathbf{O}}$ are evaluated by integration of the contact stresses over the femoral surface $\hat{\Omega}$:

$$\mathbf{f}_c = -\mathbf{R} \cdot \int\int_{\hat{\Omega}} \hat{\sigma}_n \hat{\mathbf{n}}\, d\hat{\Omega}, \tag{18a}$$

$$\mathbf{m}_c = -\mathbf{R} \cdot \int\int_{\hat{\Omega}} \hat{\sigma}_n \hat{\mathbf{e}} \times \hat{\mathbf{n}}\, d\hat{\Omega}. \tag{18b}$$

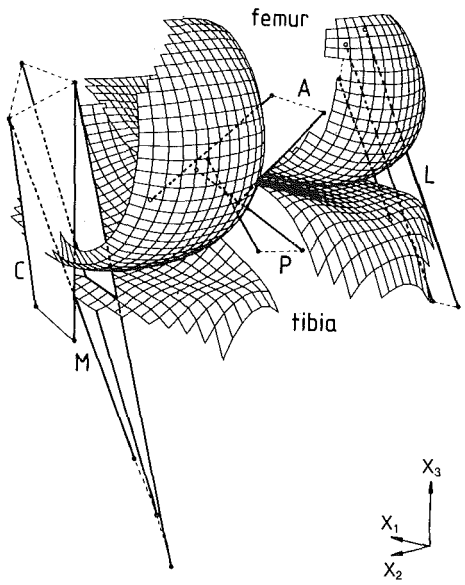

Fig. 3(*a*)

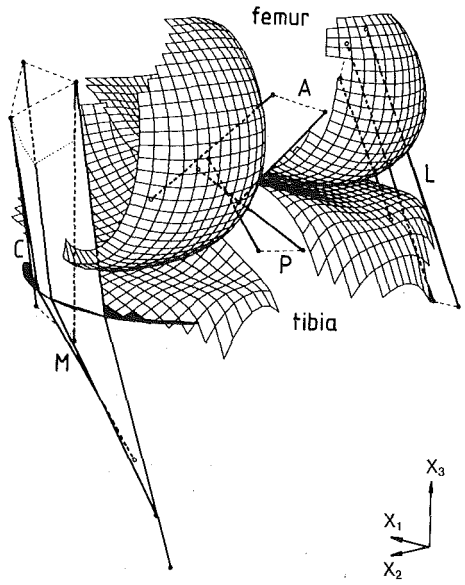

Fig. 3(*b*)

Fig. 3 Perspective views of the knee model geometry for the model without (*a*) and with (*b*) the medial bony edge for the knee in extension. *A* = anterior cruciate, *P* = posterior cruciate, *L* = lateral collateral, *M* = medial collateral, *C* = medial capsule.

in which $\hat{\mathbf{c}}$ is the location of a point $\hat{c}$ on the femoral surface and $\hat{\mathbf{n}}$ is the outward normal on the surface in point $\hat{c}$. These integrals are evaluated numerically for each iteration in the Newton-Raphson procedure (Blankevoort et al., 1991b).

The elastic modulus of the cartilage was estimated at 5 N/mm^2 and the Poisson's ratio at 0.45. This was based on a medium-to-short time response of articular cartilage to indentation (Kempson et al., 1980; Mow et al., 1982). The thickness of the tibial and the femoral articular cartilage layer were assumed to be 2 mm (Walker and Hajek, 1972; Roth, 1977).

Model Analyses. The geometrical data of a knee specimen from the experimental studies of Blankevoort et al. (1988) were used as input for the knee model. The ligaments were subdivided into two or three bundles (Fig. 3) (Blankevoort et al., 1991a). The anterior (ACL) and posterior (PCL) cruciate ligaments were modelled by two fiber bundles each, which represented the most anterior and posterior portions of each ligament. The guideline for the choice of the insertion location was the approximate elliptical shape of the femoral insertion of the ACL and PCL; the two apexes on the long axis of the elliptical shape identified the extremes of the insertion areas. The centers of the areas inside these apexes were chosen as the insertion points. The bundles originating from the femoral anterior and posterior insertions were then followed to the tibia to define the tibial insertions. The lateral collateral ligament (LCL) was modelled by three line elements which represented the most anterior, posterior, and superior bundles as identified from the femoral insertion area. Two parts of the medial collateral ligament were identified: the superficial part (MCL) represented by three line elements, and the deep part (CMCL) represented by two line elements. The three line elements of the MCL were identified from the femoral insertion area as posterior, anterior, and inferior. The two line elements of the CMCL were identified from the femoral insertion area as anterior and posterior and inserted just below the medial edge on the tibia. The geometries of the articular surfaces and the medial bony edge were measured by a stereophotogrammetric method from Meijer et al. (1988). The surface geometry data points were used to obtain the parameters for the surface polynomials of each of the four surfaces; i.e., the medial and lateral tibial plateaus and the medial and lateral femoral condyles (Blankevoort et al., 1991b). Two flexion motions were simulated. These were flexion motions with an internal or an external moment of 3 Nm applied around the x_3-axis resulting in a flexion motion combined with internal rotation for the first motion pathway and with external rotation for the second motion pathway. These motions represent motions along the so-called envelope of passive knee motion from Blankevoort et al. (1988). A second set of model evaluations was for a varus-valgus test for the joint in extension, and in 20 and 30 degrees flexion. In the varus-valgus tests, the axial rotation was restrained. Both simulations were performed twice, with and without the MCL-bone interaction. In order to test the effect of MCL pretension on the aforementioned model simulations, the simulations with MCL-bone interaction were repeated after decreasing the reference strains by 0.03 relative to the initial values (Table 1).

The varus-valgus laxity and stiffness parameters from the experiments of Markolf et al. (1978, 1984) were compared with the model evaluations of the varus-valgus laxity. For this purpose, the following parameters were calculated from the model results: the total varus-valgus laxity at 20 Nm, the varus stiffness at 10 Nm and the valgus stiffness at 10 Nm for the joint in extension, in 20 and 30 degrees flexion.

Results

The geometric configurations of the model with and without the MCL wrapping around the medial bony edge of the tibia are shown in Fig. 3 for the joint in extension. Without the MCL-bone interaction, the MCL runs through the medial tibial articular surface, and the fibers of the CMCL were located more superficially than the MCL. With the medial bony edge, the MCL was redirected in its course, and the CMCL had a more proper anatomic location relative to the MCL. Although the medial tibial edge did redirect the MCL, the MCL was not entirely free from the medial surface of the femur, because of the absence of the femoral bony edge in the model. In the simulations with the MCL-bone interaction, no signs of loosening between the MCL and the edge were noticed.

The presence or absence of the MCL-bone interaction had only little effects on the motion parameters describing flexion with an internal or an external moment of 3 Nm (Figs. 4 and 5). The internal-external rotation as function of flexion was hardly affected (Fig. 4), nor were there large changes noticed

with respect to the coupled varus-valgus rotations (Fig. 4) and proximal-distal translations. For external rotation, the redirection of the MCL caused a slight anterior shift of the femur relative to the tibia of about 1 mm over the whole flexion range and a maximal medial shift of 1.2 mm (Fig. 5). The release of the MCL by a reduction of the reference strain by 0.03, caused an increase of the external rotation of 3.5 degrees maximally at extension, in the model with the MCL-bone interaction (Fig. 4). Only slight AP-shifts were noticed. The MCL release did cause a slight lateral shift for both the internal and external motion pathways (Fig. 5).

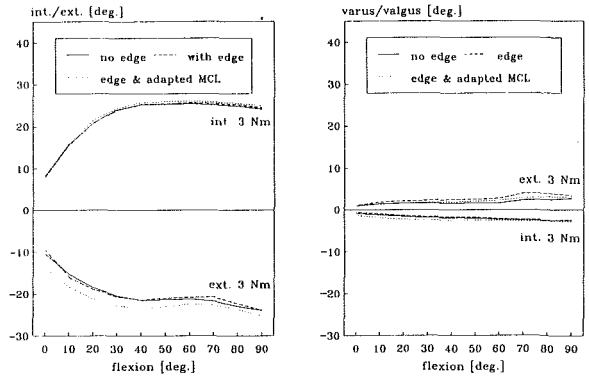

Fig. 4 The envelope of passive knee joint motion as simulated by the knee models without the medial edge (no edge), with the medial edge (with edge) and with the medial edge in combination with a release of the MCL (edge & adapted MCL). The internal motion pathway is a flexion motion with an internal moment of 3 Nm (Int. 3 Nm) and the external motion pathway is a flexion motion with an external moment of 3 Nm (Ext. 3 Nm).

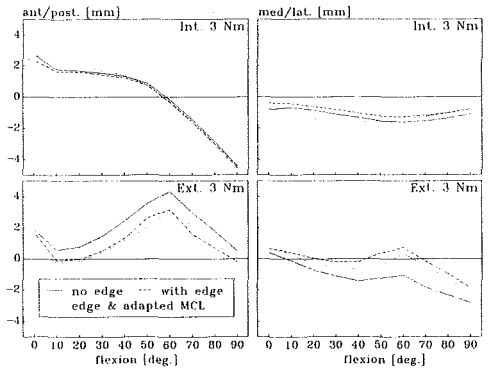

Fig. 5 The two coupled translations of the femur relative to the tibia as functions of flexion for the internal (Int. 3 Nm) and external (Ext. 3 Nm) motion pathways, which were found to be sensitive to the MCL-bone interaction: anterior-posterior translation and medial-lateral translation. The model configurations were without the medial edge (no edge), with the medial edge (with edge) and with the medial edge in combination with a release of the MCL (edge & adapted MCL).

In the varus-valgus simulations, only the valgus tests were affected by the introduction of the MCL-bone interaction and the release of the MCL (Fig. 6). The MCL is tensed in valgus and the MCL-bone interaction was shown to be of particular importance here. Redirection of the MCL caused it to counterbalance more effectively the applied valgus moment with a reduced valgus rotation. The decrease of the valgus rotation for the 24 Nm valgus moment was 0.9 and 1.7 degrees for extension and 30 degrees flexion, respectively. The release of the MCL by decreasing the reference strains increased the valgus rotations by 1.2 and 1.8 degrees maximally for extension and 30 degrees flexion, respectively. At 30 degrees flexion, the moment-rotation curves were similar for the simulation with the released MCL wrapping around the bony edge and the simulation without the edge.

The in vivo experiments of Markolf et al. (1978, 1984) concerned 49 normal subjects (normal group), which were tested only in extension, and 35 subjects with documented absence of the ACL (ACL group), which were tested in extension and 20 degrees flexion. Of the latter group, only the data of the non-injured knees are used for comparison with the present model results. Markolf et al. (1978, 1984) performed their varus-valgus tests under semi-constrained conditions, in a sense that the axial rotation was restrained. The means and standard deviations of the varus-valgus laxity and stiffness parameters of the normal and non-injured knees are listed in Table 2, and are compared with the values obtained in the model with the MCL-bone interaction and the released MCL. The model characteristics compare relatively well with the in vivo experiments, although relative to the non-injured knees of the ACL group, the varus-valgus laxity in the model for extension was somewhat higher and the stiffnesses somewhat lower. At 20 degrees flexion, the valgus stiffness in the model was a little higher than the reported experimental value. The effect of increasing the flexion angle from 20 to 30 degrees did not dramatically change the laxity parameters.

Discussion

This study was aimed at incorporating a description for a ligament wrapping around a bony edge in a three-dimensional mathematical model of the knee, and quantifying the effects on the passive motion characteristics of the knee when the MCL interacts with the medial tibial edge. The model as proposed by Hefzy and Grood (1983) for ligament-bone interaction was incorporated into a three-dimensional mathematical model of the knee-joint. In the present mathematical formulation of the knee model, where the femur is assumed to move relative to the tibia, the equations of force and moment equi-

Table 2 Comparison of varus-valgus laxity and stiffness values between the data of Markolf et al. (1978, 1984) from in vivo testing of intact knees and the present knee model including the MCL-bone interaction and the released MCL

		extension	20 deg flexion	30 deg flexion
Varus/valgus laxity at ±20 Nm	[deg]			
Markolf et al. (1978)		6.9±2.5	-	-
Markolf et al. (1984)		4.7±2.5	12.3±3.7	-
Knee model with medial edge		7.9	11.9	11.8
Varus stiffness at 10 Nm	[Nm/deg]			
Markolf et al. (1978)		6.1±4.0	-	-
Markolf et al. (1984)		9.3±5.7	3.0±1.1	-
Knee model with medial edge		5.4	3.2	3.6
Valgus stiffness at 10 Nm	[Nm/deg]			
Markolf et al. (1978)		6.1±3.6	-	-
Markolf et al. (1984)		11.0±7.3	3.0±0.8	-
Knee model with medial edge		5.7	5.1	4.9

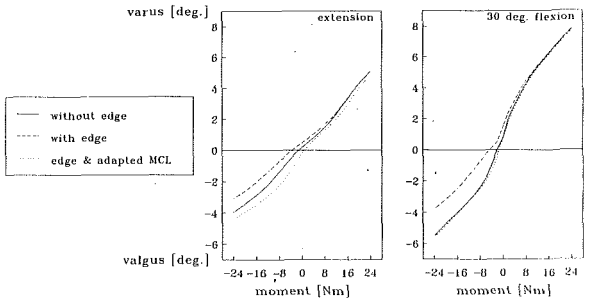

Fig. 6 The varus-valgus characteristics at extension and 30 degrees flexion for the three model configurations: without the medial edge (no edge), with the medial edge (with edge) and with the medial edge in combination with a release of the MCL (edge and adapted MCL).

librium are expressed as forces and moments acting on the femur. The wrapping of a ligament around a bony edge of the tibia, implies only a redirection of the ligament force acting on the femur. When a ligament wraps around a bony edge of the femur not only the ligament force is redirected, but also the force at the contact with the femur will participate in the equilibrium equations. In this case the mathematics of the ligament bone interaction is somewhat more complicated, particularly if it is combined with the wrapping of a ligament around a tibial bony edge. In this paper only the wrapping of a ligament around a tibial bony edge is addressed and applied to the MCL. The parametric model analyses of this interaction showed that it did not dramatically change the model characteristics with respect to forced internal-external rotations and forced varus rotations. The redirection of the MCL tensions did cause the MCL to counterbalance more effectively the forced valgus rotations. This increased effectiveness could be quantified by the reduction of the initial strain by 0.03 relative to the model without the MCL-edge, which resulted in the same valgus characteristics at 30 degrees flexion as compared to the model without the medial edge. This means that with a MCL stiffness of 8250 Newton per unit strain, a reduction of the MCL force of about 250 N is obtained for the maximum valgus moment.

The ligament reference strains of the ligament fiber bundles in the model were adapted as to match the internal and external rotation laxities of the knee specimen which was modeled on the basis of previously reported experiments (Blankevoort et al., 1988). Hence, the motion characteristics of the model for the internal and external motion pathways were very close to those of the experiments (Blankevoort et al., 1991b). Because of the small effects on these motion pathways, the match between the model and the experiments seems independent of the presence or absence of the MCL-bone interaction. Since varus-valgus tests were not included in the previously mentioned experimental study, the varus-valgus characteristics of the model with the MCL-bone interaction were compared to values as reported in the literature. The data of Markolf et al. (1978, 1984) were chosen because of the consistency of the results relative to their in vitro experiments (Markolf et al., 1976, 1981), the load-application method and the technique of measuring the relative varus-valgus rotations. The varus-valgus laxity at 20 Nm and the stiffnesses at 10 Nm of the knee model agree very well with the reported data. It must be mentioned, however, that the knee model in this study represented one individual joint specimen with estimated ligament stiffnesses and reference strains. Further model analyses, using the geometric data from more knees, are needed to substantiate the validity of the knee model in this respect.

The incorporation of a ligament wrapping around bone in a three-dimensional mathematical model of the human knee is feasible and is important with respect to those studies which are focused on mechanical aspects in which the redirection of ligaments over bony surfaces plays an important role. This is the case for the medial collateral ligament interacting with the medial bony edge of the tibia, where it concerns the forced valgus laxity, but the effects are not dramatic. The mathematical formulation of the ligament-bone interaction can also be applied, in adapted form, to the anterior cruciate ligament interacting with intercondylar notch of the femur, which may occur for extension and hyperextension of the joint.

Acknowledgment

This research program was sponsored in part by grant 90-90 from The Netherlands Organization for Research (NWO/MEDIGON). The basis of the computer programs of the knee model was developed by L. Dortmans and the model for the ligament-bone interaction was incorporated in the knee model by R.A.M. van Helvoort, both from the Faculty of Mechanical Engineering of the Eindhoven University of Technology.

References

Andriacchi, T. P., Mikosz, R. P., Hampton, S. J., and Galante, J. O., 1983, "Model Studies of the Stiffness Characteristics of the Human Knee Joint," *J. Biomechanics*, Vol. 16, pp. 23–29.

Bargar, W. L., Moreland, J. R., Markolf, K. L., Shoemaker, S. C., Amstutz, H. C., Grant, T. T., 1980, "In vivo Stability Testing of Post Meniscectomy Knees," *Clin. Orthop. Rel. Res.*, Vol. 150, pp. 247–252.

Blankevoort, L., Huiskes, R., and de Lange, A., 1984, "An in-vitro Study of the Passive Kinematic Behavior of the Human Knee-Joint," *1984 Advances in Bioengineering*, Ed. by Spilker, R. L., The American Society of Mechanical Engineers, New York.

Blankevoort, L, Huiskes, R., and de Lange, A., 1988, "The Envelope of Passive Knee Joint Motion," *J. Biomechanics*, Vol. 21, pp. 705–720.

Blankevoort, L., Huiskes, R., and de Lange, R., 1990, "Helical Axes of Passive Knee Joint Motions," *J. Biomechanics*, Vol. 23, pp. 1219–1229.

Blankevoort, L., Huiskes, R., and de Lange, A., 1991a, "Recruitment of Knee Joint Ligaments," ASME JOURNAL OF BIOMECHANICAL ENGINEERING, Vol. 113, pp. 94–103.

Blankevoort, L., Kuiper, J. H., Huiskes, R., and Grootenboer, H. J., 1991b, "Articular Contact in a Three Dimensional Model of the Knee," *J. Biomechanics* (in print).

Butler, D. L., Kay, M. D., and Stouffer, D. C., 1986, "Comparison of Material Properties in Fascicle-Bone Units from Human Patellar Tendon and Knee Ligaments," *J. Biomechanics*, Vol. 19, pp. 425–432.

Crowninshield, R., Pope, M. H., and Johnson, R. J., 1976, "An Analytical Model of the Knee," *J. Biomechanics*, Vol. 9, pp. 397–405.

Danylchuk, K., 1975, "Studies on the Morphometric and Biomechanical Characteristics of Ligaments of the Knee Joint," M.Sc. thesis, University of Western Ontario, London, Ontario, Canada.

Essinger, J. R., Leyvraz, P. F., Heegard, J. H., and Robertson, D. D., 1989, "A Mathematical Model for the Evaluation of the Behavior During Flexion of Condylar-Type Knee Prostheses," *J. Biomechanics*, Vol. 22, pp. 1229–1241.

Hefzy, M. S., and Grood, E. S., 1983, "An Analytical Technique for Modelling Knee Joint Stiffness—Part II: Geometric Non-Linearities," ASME JOURNAL OF BIOMECHANICAL ENGINEERING, Vol. 105, pp. 145–153.

Huiskes, R. Kremers, J., de Lange, A., Woltring, H. J., Selvik, G., and van Rens, Th.J.G., 1985, Analytical Stereophotogrammetric Determination of Three-Dimensional Knee-Joint Geometry," *J. Biomechanics*, Vol. 18, pp. 559–570.

Grood, E. S., and Suntay, W. J., 1983, "A Joint Coordinate System for the Clinical Description of Three Dimensional Motions: Application to the Knee," ASME JOURNAL OF BIOMECHANICAL ENGINEERING, Vol. 105, pp. 136–144.

Kempson, G. E., 1980, "The Mechanical Properties of Articular Cartilage," *The Joints and Synovial Fluid*, Vol. II, Academic Press, New York, Ed. by Sokoloff, L., pp. 177–238.

Markolf, K. L., Mensch, J. S., and Amstutz, H. C., 1976, "Stiffness and Laxity of the Knee—The Contributions of the Supporting Structures," *J. Bone and Joint Surg*, Vol. 58-A, pp. 583–594.

Markolf, K. L., Graff-Radford, A., and Amstutz, H. C., 1978, "In Vivo Knee Stability. A Quantitative Assessment Using an Instrumented Clinical Testing Apparatus," *J. Bone and Joint Surg.*, Vol. 60-A, pp. 664–674.

Markolf, K. L., Bargar, W. L., Shoemaker, S. C., and Amstutz, H. C., 1981, "The Role of Joint Load in Knee Stability," *J. Bone and Joint Surg.*, Vol. 63-A, pp. 570–585.

Markolf, K. L., Kochan, A., and Amstutz, H. C., 1984, "Measurement of Knee Stiffness and Laxity in Patients with Documented Absence of the Anterior Cruciate Ligament," *J. Bone and Joint Surg.*, Vol. 66-A, pp. 242–253.

Meijer, R. C. M. B., Huiskes, R., and Kauer, J. M. G., 1989, " A Stereophotogrammetric Method for Measurements of Ligament Structure," J. Biomechanics, Vol. 22, pp. 177–184.

Mow, V. C., Lai, W. M., and Holmes, M. H., 1982, "Advanced Theoretical and Experimental Techniques in Cartilage Research," *Biomechanics: Principles and Applications*, Ed. by Huiskes R., van Campen, D. H. and de Wijn, J. R., Martinus Nijhoff Publishers, The Hague, pp. 47–74.

Roth, V., 1977, "Two Problems in Articular Biomechanics: I. Finite Element Simulation for Contact Problems of Articulations, II. Age Dependent Tensile Properties," Ph.D. thesis Rensselaer Polytechnic Institute, Troy NY.

Walker, P. S., and Hajek, J. V., 1972, "The Load-Bearing Area in the Knee Joint," *J. Biomechanics*, Vol. 5, pp. 581–589.

Wismans, J., Veldpaus, F., Janssen, J., Huson, A., and Struben, P., 1980, "A Three-Dimensional Mathematical Model of the Knee-Joint," *J. Biomechanics*, Vol. 13, pp. 677–685.

Wismans, J., 1980, "A Three-Dimensional Mathematical Model of the Human Knee Joint," PhD thesis, Eindhoven University of Technology, Eindhoven, The Netherlands.

Woltring, H. J., 1991, "Representation and Calculation of 3-D Joint Movement," *Human Movement Sc*, Vol. 10(5) (in print).

This means that the direction of the load coincides with the direction of the constrained degree of freedom. The magnitude of the constraint loads are determined by solving the force and moment equilibrium equations (1) containing the restraint forces $\mathbf{f}_r$ and $\mathbf{m}_r$ (3).

The system used to specify the rotation matrix $\mathbf{R}$ is known as Bryant angles, where the angular orientation of the moving coordinate system is thought to be the results of three successive rotations through angles ϕ (x_3-axis), ψ (x_1-axis) and ω (x_2-axis). In this way rotation matrix $\mathbf{R}$ is

$$\mathbf{R}=\begin{bmatrix} \cos\phi\cos\omega-\sin\phi\sin\psi\sin\omega & -\sin\phi\cos\psi & \cos\phi\sin\omega+\sin\phi\sin\psi\cos\omega \\ \sin\phi\cos\omega+\cos\phi\sin\psi\sin\omega & \cos\phi\cos\psi & \sin\phi\sin\omega-\cos\phi\sin\psi\cos\omega \\ -\cos\psi\sin\omega & \sin\psi & \cos\psi\cos\omega \end{bmatrix} \tag{A9}$$

APPENDIX

Kinematic Constraints

For the evaluation of the kinematic constraints, the kinematic constraint vectors are obtained through the derivatives of the translation vector and the rotation matrix with respect to the translation and rotation components, respectively. This is performed through applying variational calculus to the kinematic equation (2):

$$\delta\mathbf{p}=\delta\mathbf{a}+\delta\mathbf{R}\cdot\hat{\mathbf{p}}. \tag{A1}$$

This can be rewritten to

$$\delta\mathbf{p}=\delta\mathbf{a}+\delta\mathbf{R}\cdot\mathbf{R}^t\cdot\mathbf{R}\cdot\hat{\mathbf{p}}. \tag{A2}$$

The rotation matrix $\mathbf{R}$ is proper orthogonal, so $\delta\mathbf{R}\cdot\mathbf{R}^t$ is skew symmetric. Vector $\delta\boldsymbol{\pi}$ exists such that for every $\mathbf{w}$ holds:

$$\delta\mathbf{R}\cdot\mathbf{R}^t\cdot\mathbf{w}=\delta\boldsymbol{\pi}\times\mathbf{w}. \tag{A3}$$

Vector $\delta\boldsymbol{\pi}$ is called the axial vector of $\delta\mathbf{R}\cdot\mathbf{R}^t$. Together with $\mathbf{R}$, this vector determines $\delta\mathbf{R}$ uniquely. The variation of the kinematic equation can be written as:

$$\delta\mathbf{p}=\delta\mathbf{a}+\delta\boldsymbol{\pi}\times(\mathbf{R}\cdot\hat{\mathbf{p}}). \tag{A4}$$

One or more of the position parameters may be prescribed. These kinematical constraints can be written as

$$k_i(\mathbf{a},\mathbf{R})=0. \tag{A5}$$

Variation of this expression yields:

$$k_i(\mathbf{a}+\delta\mathbf{a},\mathbf{R}+\delta\mathbf{R})=0. \tag{A6}$$

Using a Taylor-series expansion it can be shown that $\delta\mathbf{a}$ and $\delta\mathbf{R}$ are kinematically admissable, i.e., they do not violate the constraints if

$$\boldsymbol{\alpha}_i\cdot\delta\mathbf{a}+\boldsymbol{\beta}_i\cdot\delta\boldsymbol{\pi}=0 \tag{A7}$$

The vectors $\boldsymbol{\alpha}_i$ and $\boldsymbol{\beta}_i$ are determined uniquely by the kinematical conditions. They will be derived here for each of the degrees of freedom to be constrained. During kinematically admissable variations, i.e. variations which do not violate the constraints, no work is done by the load that is needed to retain the prescribed femoral position parameters. Hence

$$\mathbf{f}_r\cdot\delta\mathbf{a}+\mathbf{m}_r\cdot\delta\boldsymbol{\pi}=0. \tag{A8}$$

For variations $\delta\mathbf{R}$ of the rotation matrix $\mathbf{R}$, the following holds:

$$\delta\mathbf{R}=\frac{\partial\mathbf{R}}{\partial\phi}\delta\phi+\frac{\partial\mathbf{R}}{\partial\psi}\delta\psi+\frac{\partial\mathbf{R}}{\partial\omega}\delta\omega. \tag{A10}$$

The axial vector $\delta\boldsymbol{\pi}$ of the skew-symmetric matrix $\delta\mathbf{R}\cdot\mathbf{R}^t$ can then be determined, yielding

$$\delta\boldsymbol{\pi}=\begin{bmatrix} \cos\phi\,\delta\psi-\sin\phi\cos\psi\,\delta\omega \\ \sin\phi\,\delta\psi+\cos\phi\cos\psi\,\delta\omega \\ -\delta\phi+\sin\psi\,\delta\omega \end{bmatrix} \tag{A11}$$

Variations $\delta\phi$, $\delta\psi$ and $\delta\omega$ can be expressed as a function of $\delta\boldsymbol{\pi}$:

$$\delta\phi=[-\mathbf{e}_3+\tan\psi(-\sin\phi\,\mathbf{e}_1+\cos\phi\,\mathbf{e}_2)]\cdot\delta\boldsymbol{\pi}, \tag{A12a}$$

$$\delta\psi=(\cos\phi\,\mathbf{e}_1+\sin\phi\,\mathbf{e}_2)\cdot\delta\boldsymbol{\pi}, \tag{A12b}$$

$$\delta\omega=\frac{1}{\cos\psi}(-\sin\phi\,\mathbf{e}_1+\cos\phi\,\mathbf{e}_2)\cdot\delta\boldsymbol{\pi}, \tag{A12c}$$

in which $\mathbf{e}_1$, $\mathbf{e}_2$, and $\mathbf{e}_3$ are the unit vectors pointing along the corresponding coordinate axes. These relations do not hold when $\cos\psi=0$, in which case $\delta\phi$, $\delta\psi$ and $\delta\omega$ cannot be calculated from $\delta\boldsymbol{\pi}$. Then the rotation matrix $\mathbf{R}$ is called singular.

Since the three translation components (a_1,a_2,a_3) and the three rotation angles (ϕ,ψ,ω) can be prescribed, there are six possible kinematical conditions. For each of them α_j and β_j will be derived.

If a translation component a_i has a prescribed value, then δa_i has to be equal to zero. It can be concluded from (A7) that $\boldsymbol{\alpha}_j=\mathbf{e}_i$ and $\boldsymbol{\beta}_j=0$.

If the rotation angle ϕ has a prescribed value, then $\delta\phi$ has to be equal to zero. It can be concluded from (A7) and (A12*a*) that $\alpha_j=0$ and

$$\boldsymbol{\beta}_j=-\mathbf{e}_3+\tan\psi(-\sin\phi\,\mathbf{e}_1+\cos\phi\,\mathbf{e}_2) \tag{A13a}$$

If the rotation angle ψ has a prescribed value, then it follows from (A12*b*):

$$\boldsymbol{\beta}_j=\cos\phi\,\mathbf{e}_1+\sin\phi\,\mathbf{e}_2, \tag{A13b}$$

and finally for prescribing the rotation angle ω (A12*c*):

$$\boldsymbol{\beta}_j=\frac{1}{\cos\psi}(-\sin\phi\,\mathbf{e}_1+\cos\phi\,\mathbf{e}_2). \tag{A13c}$$